

D. KALISZ*

INFLUENCE OF CASTING MOLD SLAG ON THE PROGRESS OF CASTING PROCESS**WPŁYW WŁASNOŚCI ŻUŻLA KRYSZTAŁIZATOROWEGO NA PRZEBIEG PROCESU ODLEWANIA**

This paper analysis one of the basic properties of liquid slag which is viscosity. The slag in the mold fills there is between the wall and the ingot mold, where it occurs in the form of a thin layer of solidified and molten slag. The main function is to lubricate the walls of the crystallizer and control of the heat transport from the solidifying steel. The research work carried out by concentric cylinder viscosity for five samples of slag for use in industrial environments. The study was conducted for the temperature range 1200-1550°C. Then the experimental results were compared with model calculations. The differences between the experimental results and the model calculations are related to the construction of the slag and the assumptions. Measurements under laboratory conditions on the two-phase system: a liquid solution of the dispersed phase ion steel - carbon, whereas the calculation model are the liquid-phase, and therefore the viscosity calculated values are lower than the values measured.

Keywords: mold slag, continuous casting process, slag viscosity, viscosity modeling, CaO-SiO₂-Al₂O₃ slag

Obecna praca analizuje jedną z podstawowych właściwości ciekłego żużla krystalizatorowego jaką jest lepkość. Żużel w krystalizatorze wypełnia szczelinę pomiędzy ścianami krystalizatora a wlewkiem, gdzie występuje w postaci zestalonej oraz cienkiej warstwy ciekłego żużla. Główną jego funkcją jest smarowanie ścian krystalizatora oraz kontrola transportu i odprowadzania ciepła z krzepnącej stali. W pracy wykonano badania lepkości metodą koncentrycznych cylindrów dla pięciu próbek żużli stosowanych w warunkach przemysłowych. Badania przeprowadzono dla przedziału temperatur 1200-1550°C. Następnie wyniki doświadczalne porównano z obliczeniami modelowymi. Różnice pomiędzy wynikami doświadczalnymi oraz obliczeniami modelowymi związane są z budową żużli i przyjętymi założeniami. Pomiary w warunkach laboratoryjnych dotyczą układu dwufazowego: ciekły roztwór jonowy z rozproszoną fazą stałą – węglem, z kolei obliczenia modelowe odnoszą się cieczy jednofazowej, dlatego wartości obliczone lepkości mają wartości niższe od zmierzonych.

1. Introduction

In the process of steel ingot production in the continuous casting machine, the use of mold slag is necessary. Mould slag assures the control of heat flux between solidified shell of metal and the mold at the whole mold length. This allows for the elimination of longitudinal cracks in the vicinity of ingot corners. Another crucial role of mould slag is the reduction of friction between the ingot and mould walls. The liquid slag bath on the top of liquid metal plays a role of thermal insulation and protective barrier against contamination from gaseous atmosphere, like oxygen or water vapour. Carbon grains dispersed in slag float at the surface region of slag layer, where they react with oxygen. As a result protective atmosphere of CO is produced. Another important function of carbon grains appears shortly after mold powder introduction to the mold. The carbon grains position themselves among the oxide grains, what prevents their too early sintering or even melting. Only just after carbon oxidization the oxides melt together to form the mold slag in contact with liquid steel. The size distribution of carbon grains controls the rate of liquid slag formation. If

carbon is strongly particulated, during mixture softening fine droplets of liquid slag appear. Such mold powders are mainly applied at high casting rates. In turn, the mold powders with higher contribution of coarse particles are used in casting of steel liable to cracking, where casting rates are moderate or low.

At each oscillation stroke liquid slag becomes sucked into the slit between solidifying steel band and the mold wall. Up to this point the whole carbon contained in the mold powder should be oxidized. In the space between band and mold wall the slag solidifies. Solid slag layer is approximately 2 mm thick, and thin liquid layer of 0.1 mm is still present in close contact with steel band. In the time of band descending in the mold, the glassy slag transforms into crystalline form.

The liquid slag plays an important role in the process of absorption of non-metallic inclusions, which precipitate from liquid steel due to the decrease of temperature, which in turn causes the lowering of solubility product of inclusion – forming components, Micro-segregation of steel components at the

* AGH UNIVERSITY OF SCIENCE AND TECHNOLOGY, FACULTY OF FOUNDRY ENGINEERING, 30-059 KRAKÓW, 23 REYMONTA STR., POLAND

solidification front is also favorable for non-metallic inclusions formation.

Slag viscosity, temperatures of solidification beginning and ending, basicity as well as surface tension are the physico-chemical properties of casting mold slag, which predominantly affect the application of slag and its behavior in the process.

2. Subject of the study

The examinations were carried out on the mold slags obtained from mold powders. The chemical compositions of the slags under study are given in Table 1. The chemical composition of mold slag is selected appropriate to the type of steel, its melting point and viscosity. The slags presented in Table 1 are of strongly differentiated chemical composition, what influences their basicity and viscosity. Three oxides: Al_2O_3 , CaO i SiO_2 , are dominant components of slag. Their cumulative content is 66 do 75%.

TABLE 1
Chemical composition of mold slags studied in the present work
[mass %]

Slag composition [mass %]	Slag 1	Slag 2	Slag 3	Slag 4	Slag 5
SiO_2	34,4	30,9	31,9	27,5	34,2
CaO	27,0	37,5	36,4	36,5	29,1
MgO	3,9	1,0	1,2	2,75	2,6
Al_2O_3	4,7	5,9	6,2	4,5	5,7
$\text{Na}_2\text{O}/\text{K}_2\text{O}$	11,8	8,85	8,85	—	8,77
Fe_2O_3	1,6	1,2	1,0	1,5	1,5
MnO_2	—	—	0,2	—	—
Li_2O	—	—	—	—	—
B_2O_3	—	—	—	—	—
F	9,0	10,5	9,1	8,0	6,9
C dissolved.	3,6	3,8	3,5	3,25	4,3
CO_2	7,7	5,0	4,9	7,5	7,2
C total	5,7	5,2	C gaz. 4,9	5,25	—
H_2O	0,6	0,8	0,1	0,6	—
TiO_2	—	—	0,3	—	—

Fig. 1 presents the isotherms of liquidus surface for the system $\text{CaO} - \text{SiO}_2 - \text{Al}_2\text{O}_3$.

Generally the liquidus temperature is higher than 1673 K with the exception the region of composition near 30% CaO , 15% Al_2O_3 and 55% SiO_2 . To decrease the liquidus temperature, additional components are applied, mainly CaF_2 . Fig. 2 presents the liquidus surface in the system $\text{CaO} - \text{CaF}_2 - \text{SiO}_2$.

The CaF_2 addition not only decreases liquidus temperature, but also results in decrease of slag viscosity. In this system the highest liquidus temperature appears at the composition, which corresponds to crystalline phase cuspidine

$3\text{CaO}\cdot\text{SiO}_2\cdot\text{CaF}_2$. Starting from this composition, the most distinct temperature decrease appears at CaO/SiO_2 ratio close to 1:1.5.

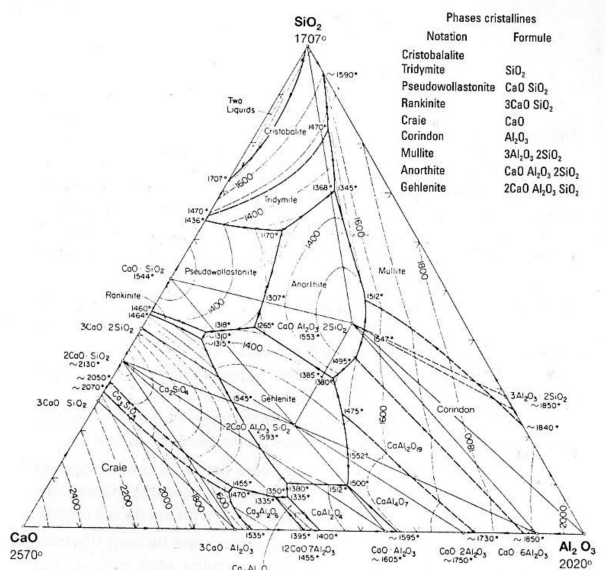


Fig. 1. $\text{CaO} - \text{SiO}_2 - \text{Al}_2\text{O}_3$ phase diagram [1]

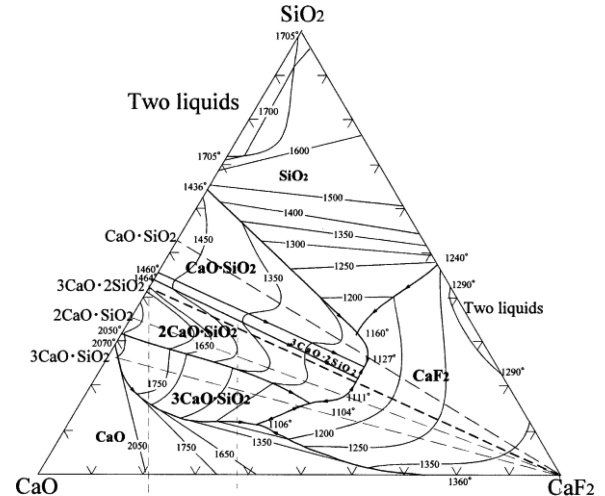


Fig. 2. $\text{CaO} - \text{SiO}_2 - \text{CaF}_2$ phase diagram [2]

The outer layer of solidified shell of steel ingot is approximately 20 mm thick. The shell thickness results from casting speed. At higher values of casting speed, where heat flow is smaller, the ingot shell is accordingly thinner. This may result in shell deformation caused with ferrostatic pressure, and, consequently, in material defects. Meng et al [2] calculated the change of ingot shell thickness in dependence on position in the mold and casting speed. The increase of casting speed results in thinner ingot shell. It may be observed that the internal mould surface, facing the ingot, has the temperature 200 do 300°C, while the temperature of outer shell surface varies from 1500 to 1100°C along band movement direction. This means, that at the distance 1-3 mm (mold slag and thin layer of gas) the temperature drops by 900-1200°C.

3. The calculation of physicochemical properties of slags under study

The mold slag components are characterized with various melting temperatures, so their mixtures melt in some temperature interval. For practical purpose the mold slag mixtures are characterized with three temperature points: denoting solidus, softening point and liquidus. In the temperature interval between solidus and liquidus the slag is the mixture of two phases: the liquid with solid particles. Cuspidyne ($3\text{CaO}\cdot\text{SiO}_2\cdot\text{CaF}_2$), which is the dominant compound of crystalline slag, has the melting temperature 1680 K. For this reason it may already form at early stage of process, in the sub-meniscus region of liquid steel. The determination of basic slag properties, like viscosity, thermal conductivity and surface tension in this region is difficult, as slag is not fully liquid. The liquidus temperature of slag, i.e. the temperature of fluidity, may be calculated from the relation [3]:

$$\begin{aligned} T_{liq}(K) = & 958 + 656,9X\text{SiO}_2 + 1040,7X\text{CaO} + 1343,2X\text{Al}_2\text{O}_3 + \\ & 1090,5X\text{MgO} + 137X\text{Na}_2\text{O} - 668X\text{K}_2\text{O} + 408,7X\text{Li}_2\text{O} + \\ & 522X\text{FeO} + 760,9\text{MnO} + 1022X\text{CrO} + 794X\text{Fe}_2\text{O}_3 + \\ & 2198X\text{Cr}_2\text{O}_3 - 532X\text{CaF}_2 + 844X\text{TiO}_2 - 12,6\text{B}_2\text{O}_3 + \\ & 1207X\text{BaO} + 1768X\text{SrO} + 2234X\text{ZrO}_2 \end{aligned} \quad (1)$$

The Table 2 below presents the calculated liquidus temperatures for the mold slags collected in Table 1.

TABLE 2
Calculated liquidus temperatures for mold slags

Temp. liquidus [°C]	slag 1	slag 2	slag 3	slag 4	slag 5
	1308	1378	1369	1305	1328

The slag layer thickness depends on the solidification temperature of slag, which may be determined from the relations [3]:

$$T_{sol}(K) = 1103 + 68,5 \cdot \ln \eta \quad (2)$$

The viscosity coefficient of slag was calculated by means of Riboud model [3,4,5,6,7,8]. This model may be applied for slags of following components' concentrations: SiO_2 (28-48%), CaO (13-52%), Al_2O_3 (0-17%), CaF_2 (0-21%), Na_2O (0-27%). The presence of other slag components were included according to the following relations:

$$\begin{aligned} X'\text{SiO}'_2 &= X\text{SiO}_2 + X\text{P}_2\text{O}_5 + X\text{TiO}_2 + X\text{ZrO}_2 \\ X'\text{CaO}' &= X\text{CaO} + X\text{MgO} + X\text{FeO} + X\text{Fe}_2\text{O}_3 + \{X\text{MnO} + X\text{NiO} \\ &+ X\text{CrO} + X\text{ZnO} + X\text{Cr}_2\text{O}_3\} \\ X'\text{Al}_2\text{O}'_3 &= X'\text{Al}_2\text{O}'_3 + \{X'\text{B}_2\text{O}'_3\} \\ X\text{CaF}_2 & \\ X'\text{Na}_2\text{O}' &= X\text{Na}_2\text{O} + X\text{K}_2\text{O} + \{X\text{Li}_2\text{O}\} \end{aligned} \quad (3)$$

The viscosity coefficient is calculated from the relation:

$$\eta(\text{Pa} \cdot \text{s}) = A \cdot T \cdot \exp(B/T) \quad (4)$$

where:

$$\begin{aligned} A = & \exp(-19.81 + 1.73X'\text{CaO}' + 5.82X\text{CaF}_2 + 7.02X'\text{Na}_2\text{O}' \\ & - 35.76X\text{Al}_2\text{O}_3) \end{aligned} \quad (5)$$

$$\begin{aligned} B = & 31140 - 23896X'\text{CaO}' - 46356X\text{CaF}_2 - 39159X'\text{Na}_2\text{O}' \\ & + 68833X'\text{Al}_2\text{O}'_3 \end{aligned} \quad (6)$$

The A and B parameters were calculated for the Arrhenius equation [9, 10, 11]. Model Riboud'a calculated the effect of adding CaF_2 and temperature on the viscosity of slag (Table 1). The using for calculated slags are system consisting CaO , SiO_2 , Al_2O_3 , Na_2O with variable amounts 0-14% mass CaF_2 . The results of the model calculations are shown in Tables 3-7.

TABLE 3
Calculated values of dynamic viscosity coefficient [$\text{Pa} \cdot \text{s}$] for slag 1 consists CaF_2

Temp. [°C]	CaF ₂ [% mass]							
	0	2	4	6	8	10	12	14
1200	0,711	0,505	0,363	0,264	0,194	0,145	0,109	0,083
1250	0,484	0,348	0,254	0,187	0,140	0,105	0,08	0,062
1300	0,338	0,246	0,182	0,136	0,103	0,078	0,06	0,046
1350	0,241	0,178	0,133	0,101	0,077	0,059	0,046	0,036
1400	0,175	0,131	0,099	0,076	0,058	0,045	0,036	0,028
1450	0,131	0,099	0,075	0,058	0,045	0,035	0,028	0,022
1500	0,989	0,075	0,058	0,045	0,036	0,028	0,022	0,018
1550	0,076	0,058	0,049	0,036	0,028	0,023	0,018	0,015

TABLE 4
Calculated values of dynamic viscosity coefficient [$\text{Pa} \cdot \text{s}$] for slag 2 consists CaF_2

Temp. [°C]	CaF ₂ [% mass]							
	0	2	4	6	8	10	12	14
1200	0,256	0,191	0,144	0,109	0,084	0,065	0,051	0,040
1250	0,179	0,135	0,103	0,079	0,062	0,048	0,038	0,031
1300	0,129	0,098	0,076	0,059	0,046	0,037	0,029	0,023
1350	0,094	0,073	0,057	0,045	0,036	0,028	0,023	0,018
1400	0,070	0,055	0,043	0,034	0,027	0,022	0,018	0,015
1450	0,053	0,042	0,034	0,027	0,022	0,018	0,014	0,012
1500	0,041	0,033	0,027	0,022	0,017	0,014	0,011	0,009
1550	0,032	0,026	0,021	0,017	0,014	0,012	0,009	0,008

TABLE 5
Calculated values of dynamic viscosity coefficient [Pa· s] for slag 3
consists CaF₂

Temp. [°C]	CaF ₂ [%mass]							
	0	2	4	6	8	10	12	14
1200	0,319	0,237	0,178	0,135	0,103	0,080	0,062	0,049
1250	0,221	0,167	0,127	0,097	0,075	0,059	0,046	0,037
1300	0,157	0,120	0,092	0,071	0,056	0,044	0,035	0,028
1350	0,114	0,088	0,068	0,053	0,042	0,034	0,027	0,022
1400	0,084	0,066	0,052	0,041	0,032	0,026	0,021	0,017
1450	0,064	0,050	0,040	0,032	0,025	0,021	0,017	0,014
1500	0,049	0,039	0,031	0,025	0,020	0,016	0,014	0,011
1550	0,038	0,031	0,024	0,020	0,016	0,013	0,011	0,009

TABLE 6
Calculated values of dynamic viscosity coefficient [Pa· s] for slag 4
consists CaF₂

Temp. [°C]	CaF ₂ [% mass]							
	0	2	4	6	8	10	12	14
1200	0,154	0,114	0,085	0,064	0,049	0,038	0,029	0,023
1250	0,111	0,083	0,063	0,048	0,037	0,029	0,022	0,018
1300	0,082	0,062	0,047	0,036	0,028	0,022	0,018	0,014
1350	0,061	0,047	0,036	0,028	0,022	0,018	0,014	0,011
1400	0,047	0,036	0,028	0,022	0,018	0,0145	0,011	0,009
1450	0,036	0,028	0,022	0,018	0,014	0,011	0,009	0,007
1500	0,029	0,023	0,018	0,014	0,012	0,009	0,008	0,006
1550	0,023	0,018	0,015	0,012	0,009	0,008	0,006	0,005

TABLE 7
Calculated values of dynamic viscosity coefficient [Pa· s] for slag 5
consists CaF₂

Temp. [°C]	CaF ₂ [%mass]							
	0	2	4	6	8	10	12	14
1200	0,667	0,479	0,348	0,256	0,190	0,143	0,108	0,083
1250	0,451	0,328	0,242	0,180	0,136	0,103	0,079	0,061
1300	0,313	0,231	0,172	0,130	0,099	0,076	0,059	0,046
1350	0,222	0,166	0,125	0,096	0,074	0,057	0,045	0,035
1400	0,161	0,122	0,093	0,072	0,056	0,044	0,035	0,028
1450	0,119	0,091	0,070	0,055	0,043	0,034	0,027	0,022
1500	0,090	0,069	0,054	0,043	0,034	0,027	0,022	0,017
1550	0,069	0,054	0,042	0,033	0,027	0,021	0,017	0,014

For verify the results of calculations performed experimental viscosity measurements use of concentric cylinders method.

4. Examination of slag viscosity

The coefficients of dynamic viscosity of mold slags were determined with the use of concentric cylinders method. The Fig. 3 below presents the scheme of experimental arrangement.

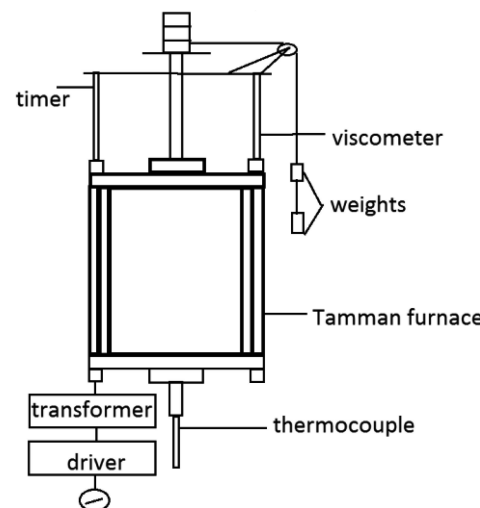


Fig. 3. Schematic view of experimental arrangement for viscosity determination

The graphite crucible of 27 mm internal diameter functioned as the outer cylinder of experimental apparatus. The crucible was placed inside the Tamman furnace. As an internal rotating cylinder the 10 mm graphite rod was applied. The slag samples of the mass 35 g were placed in graphite crucible and heated to 1550°C. The slags presented in Table 1 were the subject of the experimental investigations. For each slag composition a series of 10 measurements was carried out. In each single measurement 10 cylinder rotations were made. The temperature range under study was 1200-1550°C, with 50°C intervals. During the experiments the graphite rod was immersed in molten slag to the depth 30 mm.

The measurements were started at the temperature, at which the slag was completely liquid. This temperature results from the chemical composition, that's why the values for various samples differ considerably. In the measurements the time of one rotation was determined. Tables 8-12 below contain the results of the measurements, i.e. the values of time of one rotation of graphite rod.

TABLE 8
The results of rotation time [s] measurements for slag 1

Measur. number	1200 °C	1250 °C	1300 °C	1350 °C	1400 °C	1450 °C	1500 °C	1550 °C
1	0,341	0,271	0,254	0,245	0,229	0,224	0,222	0,221
2	0,326	0,273	0,253	0,239	0,231	0,225	0,223	0,216
3	0,308	0,272	0,260	0,242	0,232	0,224	0,222	0,221
4	0,301	0,280	0,247	0,243	0,233	0,225	0,223	0,221
5	0,297	0,266	0,254	0,242	0,236	0,226	0,225	0,220
6	0,295	0,266	0,250	0,243	0,229	0,226	0,225	0,230
7	0,288	0,263	0,250	0,241	0,234	0,219	0,225	0,220
8	0,289	0,266	0,243	0,241	0,229	0,220	0,226	0,219
9	0,286	0,258	0,249	0,239	0,234	0,224	0,222	0,220
10	0,283	0,264	0,247	0,242	0,235	0,224	0,224	0,220
Average	0,301	0,267	0,250	0,241	0,232	0,223	0,233	0,220

TABLE 9

The results of rotation time [s] measurements for slag 2

Measurement number	1300 °C	1350 °C	1400 °C	1450 °C	1500 °C	1550 °C
1	0,298	0,252	0,246	0,239	0,228	0,223
2	0,279	0,258	0,237	0,234	0,224	0,221
3	0,268	0,250	0,241	0,250	0,222	0,221
4	0,260	0,245	0,240	0,237	0,223	0,228
5	0,289	0,256	0,238	0,235	0,233	0,226
6	0,270	0,246	0,239	0,230	0,222	0,225
7	0,271	0,246	0,234	0,234	0,228	0,225
8	0,270	0,246	0,239	0,239	0,230	0,224
9	0,275	0,251	0,240	0,234	0,231	0,223
10	0,280	0,251	0,239	0,233	0,228	0,228
Average	0,276	0,2501	0,2393	0,2365	0,2269	0,2244

TABLE 10

The results of rotation time [s] measurements for slag 3

Measurement number	1300 °C	1350 °C	1400 °C	1450 °C	1500 °C	1550 °C
1	0,239	0,234	0,222	0,222	0,222	0,217
2	0,238	0,234	0,221	0,228	0,219	0,217
3	0,240	0,232	0,222	0,221	0,222	0,217
4	0,241	0,231	0,226	0,216	0,220	0,222
5	0,240	0,230	0,228	0,221	0,216	0,219
6	0,239	0,238	0,229	0,220	0,217	0,218
7	0,247	0,231	0,222	0,217	0,222	0,217
8	0,240	0,231	0,230	0,219	0,219	0,218
9	0,239	0,230	0,226	0,220	0,222	0,219
10	0,239	0,231	0,228	0,225	0,221	0,217
Average	0,2402	0,2322	0,2254	0,2209	0,2198	0,2179

TABLE 11

The results of rotation time [s] measurements for slag 4

Measurement number	1450 °C	1500 °C	1550 °C
1	0,319	0,294	0,244
2	0,317	0,255	0,238
3	0,322	0,270	0,244
4	0,328	0,274	0,244
5	0,319	0,264	0,239
6	0,320	0,266	0,244
7	0,327	0,270	0,243
8	0,328	0,261	0,238
9	0,332	0,26	0,239
10	0,323	0,27	0,241
Average	0,3235	0,2684	0,2414

TABLE 12

The results of rotation time [s] measurements for slag 5

Measurement number	1400 °C	1450 °C	1500 °C	1550 °C
1	0,271	0,259	0,249	0,230
2	0,278	0,254	0,244	0,233
3	0,265	0,254	0,245	0,236
4	0,274	0,248	0,246	0,228
5	0,271	0,253	0,244	0,229
6	0,268	0,247	0,242	0,232
7	0,270	0,253	0,228	0,231
8	0,270	0,248	0,227	0,232
9	0,265	0,252	0,245	0,229
10	0,272	0,247	0,246	0,229
Average	0,2704	0,2515	0,2416	0,2309

The expected value of viscosity coefficient is the arithmetic mean for the series of experimental results. On the basis of equation 4 (7) the coefficients of dynamic viscosity of investigated mold slags were determined as the function of temperature.

$$\eta = 102,46 (t - t_0) + 0,8842 \quad (7)$$

where:

t – time of one rotation of inner cylinder in liquid slag sample

t_0 – time of one rotation of cylinder (0.218 s)

In the Tables 13-17 the calculated values of dynamic viscosity coefficients for corresponding slags are presented.

TABLE 13

Calculated values of dynamic viscosity coefficient [Pa· s] for slag 1

Measur. number	1200 °C	1250 °C	1300 °C	1350 °C	1400 °C	1450 °C	1500 °C	1550 °C
1	1,348	0,63	0,457	0,365	0,201	0,149	0,149	0,149
2	1,194	0,651	0,447	0,303	0,221	0,160	0,129	0,119
3	1,010	0,641	0,518	0,334	0,231	0,149	0,139	0,067
4	0,938	0,723	0,385	0,344	0,242	0,160	0,129	0,119
5	0,897	0,580	0,457	0,334	0,272	0,170	0,139	0,119
6	0,877	0,580	0,416	0,344	0,201	0,170	0,160	0,108
7	0,805	0,549	0,416	0,324	0,252	0,098	0,160	0,211
8	0,815	0,580	0,344	0,324	0,201	0,108	0,160	0,108
9	0,785	0,498	0,406	0,303	0,252	0,149	0,170	0,098
10	0,754	0,559	0,385	0,334	0,262	0,149	0,129	0,108
Aver	0,942	0,599	0,423	0,331	0,233	0,146	0,146	0,122

TABLE 14
Calculated values of dynamic viscosity coefficient [Pa· s] for slag 2

Measurement number	1300 °C	1350 °C	1400 °C	1450 °C	1500 °C	1550 °C
1	0,908	0,436	0,375	0,303	0,190	0,139
2	0,713	0,498	0,283	0,252	0,149	0,119
3	0,600	0,416	0,324	0,416	0,129	0,119
4	0,518	0,365	0,313	0,283	0,139	0,190
5	0,815	0,477	0,293	0,262	0,242	0,170
6	0,621	0,375	0,303	0,211	0,129	0,160
7	0,631	0,375	0,252	0,252	0,190	0,160
8	0,621	0,375	0,303	0,303	0,211	0,149
9	0,672	0,426	0,313	0,252	0,221	0,139
10	0,723	0,426	0,303	0,242	0,190	0,190
Average	0,682	0,417	0,306	0,277	0,178	0,153

TABLE 15
Calculated values of dynamic viscosity coefficient [Pa· s] for slag 3

Measurement number	1300 °C	1350 °C	1400 °C	1450 °C	1500 °C	1550 °C
1	0,303	0,252	0,129	0,129	0,098	0,078
2	0,293	0,252	0,119	0,190	0,129	0,078
3	0,313	0,231	0,129	0,119	0,108	0,108
4	0,324	0,221	0,170	0,067	0,067	0,098
5	0,313	0,211	0,190	0,119	0,078	0,088
6	0,303	0,293	0,201	0,108	0,108	0,078
7	0,385	0,221	0,129	0,078	0,098	0,088
8	0,313	0,221	0,211	0,098	0,129	0,098
9	0,303	0,211	0,170	0,108	0,119	0,078
10	0,303	0,221	0,190	0,129	0,078	0,078
Average	0,315	0,233	0,164	0,115	0,101	0,087

TABLE 16
Calculated values of dynamic viscosity coefficient [Pa· s] for slag 4

Measurement number	1450 °C	1500 °C	1550 °C
1	1,123	0,867	0,354
2	1,102	0,467	0,293
3	1,154	0,621	0,354
4	1,215	0,662	0,354
5	1,123	0,559	0,303
6	1,133	0,580	0,354
7	1,205	0,621	0,344
8	1,215	0,528	0,293
9	1,256	0,518	0,303
10	1,164	0,621	0,324
Average	1,169	0,604	0,328

TABLE 17
Calculated values of dynamic viscosity coefficient [Pa· s] for slag 5

Measurement number	1400 °C	1450 °C	1500 °C	1550 °C
1	0,631458	0,508506	0,406046	0,211372
2	0,703180	0,457276	0,354816	0,242110
3	0,569982	0,457276	0,365062	0,272848
4	0,662196	0,395800	0,375308	0,190880
5	0,631458	0,447030	0,354816	0,201126
6	0,600720	0,385554	0,334324	0,231864
7	0,621212	0,447030	0,190880	0,221618
8	0,621212	0,395800	0,180634	0,231864
9	0,569982	0,436784	0,365062	0,201126
10	0,641704	0,385554	0,375308	0,201126
Average	0,62531	0,431661	0,330226	0,220593

5. Conclusions

Slags 1 and 5 contain more CaO than SiO₂. Figure 1 placed on the equilibrium diagram suggests that area with lowest melting temperatures below 1600°C in the range 43-63% mol. SiO₂, it is corresponding to 44,7-64,6% SiO₂ [13, 14, 15]. Slags 2, 3, 4, with the lowest SiO₂ content located near the lower end of this range.

CaF₂ is used to improve liquidity slag by reducing its viscosity and melting point. Riboud empirical model allowed the estimation of the effect of temperature and the viscosity of the additive CaF₂ mold slag investigated. The calculation results are different from the data obtained during the experiment was carried out. The largest difference occurs in the case of sample no. 4 of the slag. The reasons for these differences are due to configurations made in the calculation, which only roughly correspond to the actual configurations of the slag. The molten slag is crystallizers biphasic mixture, which is higher in viscosity due to the presence of solid particles. On the other side, the calculations assumed that the slag is a single-phase system this is probably due to discrepancies between the results of model calculations and experiment. The calculations also show that the addition of CaF₂ and the presence of Na₂O in the slag have the biggest effect on reducing the viscosity of the slag. This effect is particularly pronounced for samples 3 and 4 of the slag with high content of CaO to SiO₂ ratio.

Acknowledgements

This work was sponsored by Ministry of Science as the statute work at AGH University of Science and Technology in the year 2012 (contract: 11.11.170.318).

REFERENCES

- [1] G. Eriksson, A.D. Peltton, Critical Evaluation and Optimisation of the Thermodynamic Properties and Phase Diagrams of the CaO – Al₂O₃, Al₂O₃ – SiO₂ and CaO – SiO₂ – Al₂O₃ Systems, Met. Mater. Trans. B **24B**, 807-816 (1993).
- [2] Y.A. Meng, B.G. Thomass, Modelling Transient Slag – Layer Phenomena in the Shell – Mold Gap in Continuous Casting of Steel, Met. Materials Trans. B **34B**, 707-725 (2003).
- [3] K. Mills, The Estimation of Slag Properties, Short course presented as part of Southern African Pyrometallurgy (2011).
- [4] B. Zhao, S.P. Vanka, B.G. Thomass, Numerical study of flow and heat transfer in a molten flux layer, Heat and Fluid Flow **26**, 105-118 (2005).
- [5] K.C. Mills, L. Yuan, R.T. Jones, Estimating the physical properties of slags, The Journal of The Southern African Institute of Mining and Metallurgy **10**, 649-658 (2011).
- [6] Y. Meng, B.G. Thomass, A.A. Polycarpou, A. Prasad, H. Heinrich, Mould Slag Property Measurements to Characterize CC Mould – Shell Gap Phenomena, Canadian Metallurgical Quarterly **45**, 1, 79-94 (2006).
- [7] Paavo Hooli, Doctoral Thesis, Helsinki University of Technology, Department of Materials Science and Engineering, TKK-MT-195, Espoo 2007.
- [8] Lasse Forsbacka, Doctoral Thesis, Helsinki University of Technology, Department of Materials Science and Engineering, TKK-MT-196, Espoo 2007.
- [9] A. Kondratiev, P. Hayes, E. Jak, Development of Quasi – Chemical Viscosity Model for Fully Liquid Slags in the Al₂O₃ – CaO – FeO – MgO – SiO₂ System, ISIJ Intern. **46**, 359-367 (2006).
- [10] W.L. McCaulley, D. Apelian, Viscosity of Fluxes for the Continuous Casting of Steel. Materials Engineering, Drexel University, Philadelphia, PA, 19104, www.anl.gov?PCS/.../29_4_PHILADELPHIA_08-84_0151.pdf.
- [11] A.I. Zaitsev, N.V. Korolyov, B.M. Mogutnov, Phase Equilibria In the CaF₂-Al₂O₃-CaO System, Journal Mat. Sc. (rus) **26**, 1588-1600 (1991).
- [12] Z. Kalicka, E. Kawecka-Cebula, K. Pytel, Application of the Iida Model for Estimation of Slag viscosity for Al₂O₃ – Cr₂O₃ – CaO – CaF₂ Systems. Arch. Met. Materials **54**, 179-187 (2008).
- [13] L. Codourier, D.W. Hopkins, I. Wilkommiski, Fundamentals of Metallurgical Processes Pergamon Press London, New York, Toronto (1978).
- [14] E.T. Turkdogan, Physicochemical properties of molten slags and glasses, The Metals Society (1983).
- [15] T. Rosenquist, Principles of Extractive Metallurgy (1974).

Received: 15 January 2012.